The EuroBiotech Journal
RESEARCH ARTICLE
Medical Biotechnology

In Silico Analysis of Ergosterol as Antiviral Agents Targeting Monkeypox Methyltransferase, Phosphatase and A42R Profilin-like Protein Receptors

Sibel Kaymak[1*], Nilüfer Vural[1,2,] Hatice Tosyagülü Çelik[3]

Abstract

Phytosterols derived from medicinal mushrooms have emerged as promising therapeutic agents due to their high pharmacological effects, low toxicity, and high bioavailability. The increased concern about virus spread and treatment strategies following the pandemic has necessitated the discovery of new antiviral agents against various concerning viral species. This study investigated the inhibitory effects of ergosterol and its derivative phytosterols on monkeypox target proteins through in silico methods. For comparative analysis, two FDA-approved monkeypox drugs, Tecovirimat and Cidofovir, were used as controls. Key findings revealed that β-ergosterol effectively inhibited the methyltransferase VP39 protein with a binding affinity of -8.9 kcal/mol. Ergosterol peroxide showed the highest affinity for the A42R profilin-like protein, with a binding score of -8.1 kcal/mol, while ergosterol exhibited strong binding with phosphatase, also at -8.1 kcal/mol. These findings indicate that these phytosterols may serve as antiviral agents due to their comparable binding affinities. Compared to the control groups, ergosterol and its derivatives demonstrated significant in silico antiviral activity against monkeypox. Further preclinical studies, including experimental validation, are recommended to confirm these findings and explore their therapeutic potential.

Keywords: Monkeypox, Phytosterols, Ergosterol, Medicinal mushrooms, In silico

Introduction

Although it was first reported in a nine-month-old male infant in the Democratic Republic of the Congo in the 1970s, the monkeypox is believed to have been infecting humans in sub-Saharan Africa for thousands of years (Zahmatyar et al., 2023). The first outbreak occurred in the United States in 2003 and was linked to prairie dogs and Gambian rats imported from Ghana (Reynolds et al., 2007). The virus is typically transmitted through contact with the body fluids of an infected animal or via animal bites. Numerous wild animal species in Africa, including squirrels, mice, and monkeys, have shown evidence of the monkeypox virus or infection. However, the primary reservoir of the virus remains still unclear. It is believed that humans and monkeys are incidental hosts, with rodents serving as the natural host and facilitating transmission to other animals (Mitjà et al., 2023). Clinical symptoms following exposure, particularly after invasive exposures, suggest that the risk of developing systemic disease is higher when an individual touches an infected animal, comes into contact with skin or mucosal lesions, cleans an infected animal's cage, or is bitten or scratched by the animal (Farahat et al., 2022). Human-to-human transmission occurs through interaction with infected skin lesions and body fluids. The risk of transmission is higher in cases of compromised skin integrity or mucosal lesions. The frequent emergence of disease beyond Africa in recent years underscores its global significance and highlights the urgency of developing alternative treatments (Bunge et al., 2022).

The monkeypox virus is a member of the Orthopoxvirus genus within the Poxviridae family, which includes Variola, Cowpox, and Vaccinia viruses. It is a rare zoonotic

[1]Department of Biotherapeutic Products Research and Development Program, Public Health Institute, Ankara Yildirim Beyazit University, Ankara, Turkey
[2]Department of Food Processing, Health Services of Vocational School, Ankara Yıldırım Beyazit University, Ankara, Turkey
[3]Department of Plant and Animal Production, Health Services of Vocational School, Ankara Yıldırım Beyazit University, Ankara, Turkey

***Corresponding author:**
Sibel KAYMAK (sibelkaymak@aybu.edu.tr)

DOI: 10.2478/ebtj-2025-0014

viral agent that causes monkeypox disease (Martín-Delgado et al., 2022). The Poxviridae family is an ancient group of viruses known to cause 'pox' diseases before the divergence of vertebrates and invertebrates, and it is found in insects, reptiles, birds, and mammals. All virus species within this family share similar antigens, leading to cross-reactivity, and have a similar DNA sequence. Variola and Vaccinia viruses are the closest known relatives of the monkeypox virus, with genome sequences showing a high degree of similarity (96%) (Li et al., 2010). Poxviruses are among the largest and most complex known viruses. They are pleomorphic, brick-shaped viruses with a linear double-stranded DNA genome, surrounded by a lipoprotein envelope. Monkeypox virus is approximately 200-250 nanometers in size and has a biconcave, dumbbell-shaped core. Inside the core, the viral genome is located along with a DNA-protein complex and viral enzymes, which together form the nucleocapsid structure (Brennan et al., 2023). The nucleocapsid is surrounded by a lipid envelope containing tubular proteins. Members of the poxvirus family have a genome size ranging from 200-500 kb, with 150-200 genes located on both DNA strands. These genes encode products that help the virus evade host defense mechanisms, including inhibiting apoptosis, preventing antigen presentation and recognition, and disrupting interferon and signaling pathways triggered by immunostimulatory cytokines. Unlike other DNA viruses Monkeypox viruses mutate far less frequently than RNA viruses (such as Hepatitis C or SARS-CoV-2) due to the higher stability of double-stranded DNA and the 3'-5' exonuclease proofreading activity of DNA polymerase (Woolhouse et al., 2016). In addition to the high stability of its genome structure, like other viruses, Monkeypox also utilizes the host cell to replicate and survive. Some of the key protein structures involved in Monkeypox viral pathogenesis include A42R Profilin-like Protein, methyltransferase VP39, and phosphatase. A42R Profilin-like Protein aids in actin polymerization for viral assembly and manipulation of host cells (Minasov et al., 2022), while methyltransferase VP39 ensures stability and efficient replication of the viral genome through RNA methylation (Škvára 2024). The phosphatase enzyme is crucial for regulating signaling pathways that facilitate viral entry, replication, and immune evasion (Bottini et al., 2023). Together, these proteins contribute to viral replication and resistance to host immune responses, highlighting their potential as therapeutic targets in the fight against monkeypox. Recent scientific research has demonstrated that in silico analyses, utilizing intelligent algorithms provides a rapid and economic platform for screening bioactive compounds derived from plants, animals, insects, or fungi with therapeutic potential. This approach is particularly effective in discovering new drugs and inhibitor molecules targeting the molecular structures of viruses, including SARS-CoV-2, HIV, and Ebolavirus. There is no specific FDA-approved treatment for monkeypox; however, the drugs Tecovirimat, Brincidofovir, and Cidofovir are known to be used to alleviate symptoms and support recovery in patients. However, antiviral treatment strategies still face significant challenges, particularly in addressing emerging and re-emerging viral infections. Traditional antiviral drugs are often constrained by issues such as target specificity, adverse side effects, and the rapid development of drug resistance, highlighting the urgent need for novel therapeutic agents with broad-spectrum efficacy and minimal toxicity. In traditional medicine systems, particularly in the Indian Ayurvedic and Traditional Chinese Medicine, plants, animal products, mushrooms, and plant-based compounds are widely used for the treatment and management of various viral and other diseases (Talwar et al., 2020; Eng et al., 2019). Plant and mushroom extracts contain a wide range of bioactive compounds that exhibit antiviral effects, proteins, dietary fiber, vitamins, minerals, polysaccharides, terpenoids, polyphenols, alkaloids, lactones, and sterols (Taofiq et al., 2016). Furthermore, it has been found that mushroom-based drugs have been tested in human trials and have shown promising results against SARS-CoV-2 (Baruah et al., 2023). Among these bioactive compounds, phytosterols have emerged as particularly promising candidates. Derived from natural sources, these compounds are distinguished by their low toxicity, high bioavailability, and diverse biotherapeutic effects. Their unique chemical structures and mechanisms of action position them not only as potential integratives to conventional antiviral agents but also as innovative solutions to bridge existing treatment gaps.

So, the aim of this study was to investigate the antiviral potential of various ergosterol derivatives obtained from mushroom species such as *Lentinula edodes* and *Pleurotus ostreatus* (Hu et al., 2020). Ergosterol is the most abundant phytosterol in the fungal cell membrane. Similar to cholesterol in animal cell membranes, it maintains membrane integrity in fungi (Choy et al, 2023). This compound contains three double bonds at positions 5, 7, and 22, and β-hydroxy groups within a 1,2-cyclopentanoperhydrophenanthrene ring core (Figure 1), which allows it to act as an amphipathic lipid (Rangsinth et al., 2023). Ergosterol can exist in both free and esterified forms and undergoes photolysis when exposed to ultraviolet light (280–320 nm). During photolysis, it converts into pre-vitamin D2 (pre-ergocalciferol), followed by thermal conversion into vitamin D2 (ergocalciferol), which is important for human nutrition (Villares et al., 2012). Different derivatives of ergosterol can be found in various species of mushrooms and plants, and they all undergo a series of biosynthetic processes that ultimately result in products related to vitamin D. Quantitative analyses conducted on various mushrooms (*Pleurotus eryngii, Agaricus bisporus, Pleurotus ostreatus*) have shown that the amount of ergosterol and its derivative compounds ranges between 350-500 mg per 100 grams (Hammann et al., 2016). In addition to its antifungal, antiinflammatory, and antioxidant properties, ergosterol and its derivatives exhibit hypocholesterolemic, antitumor, and immunomodulatory effects. These compounds have the potential to improve cardiovascular health by regulating cholesterol metabolism. They also offer a wide range of medical applications, as they may inhibit the growth

of certain cancer cells and enhance the immune response (Andrade et al., 2019). In the present study, we evaluated ergosterol and its derivatives as potential drugs against the monkeypox virus. These predominantly mushroom-derived phytosterols, along with FDA-approved drugs as positive controls, were screened against monkeypox-specific receptor binding sites using molecular docking studies.

Materials and Methods

2.1 Phytosterol retrieval

Chemical, structural and Simplified Molecular Input Line Entry System (SMILES) data of the phytosterol molecules (ligands) were retrieved from the PubChem database (https:// pubch em. ncbi. nlm. nih. gov/). Using the SMILES data, SDF and MOL files of the phytosterol compounds were acquired by the Swiss Target Prediction server and their 3D structures were predicted (Daina et al. 2017). These phytosterol compounds are: Ergosterol, α-Dihydroergosterol, β-ergosterol, 10-α-ergosterol, 9-α,10-β-methyl ergosterol, ergosterol peroxide (Fig. 1). Tecovirimat and cidofovir were used as positive controls (Rani et al., 2024).

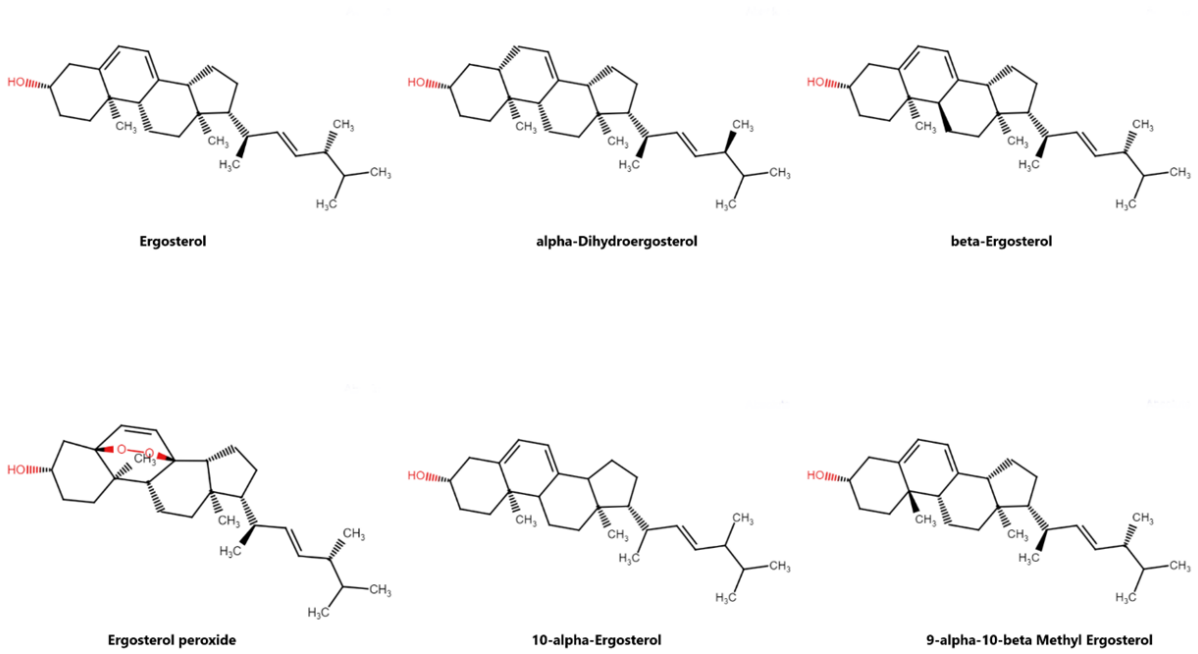

Figure 1. 2D structures of ergosterol and derivative phytosterols

2.2 Receptor protein preparation

The crystal structures of A42R Profilin-like Protein (PDB ID: 4QWO), methyltransferase VP39 (PDB ID: 8CEQ) and phosphatase (PDB ID: 8GZ4) were used as target receptors in this study. The 3D structures of the target proteins were retrieved from the Protein Data Bank (PDB) (http:// www. rcsb. org/ pdb) (Burley et al., 2017). A42R Profilin-like Protein of the monkeypox virus encoded by the gp153 locus and it directly impacts the virus's ability to infect. Researchers emphasize that this protein would be a critical target in the possible event of a monkeypox outbreak. The methyltransferase, which plays a critical role in the RNA synthesis stages of monkeypox, is involved in the encoding of certain enzymes that inhibit the host's antiviral response. This makes it an attractive target for research into therapeutic effects against the virus (Silhan et al., 2023). Lastly, phosphatases play a critical role in the replication process of the monkeypox virus and in evading host cell defense mechanisms. It is suggested that the inhibition of phosphatases could prevent the virus from replicating and suppressing the immune system (Cui et al., 2023).

2.3 3D structure configuration prediction and validation

The 3D structural models of monkeypox receptor proteins were generated using the GalaxyWeb web-tool (Heo et al., 2013). This analysis was performed based on the coordinates between the target proteins and template data. The method employed is based on Support Vector Machines (SVM), a supervised machine learning algorithm that provides secondary structure quality estimation (QSQE) by integrating interface protection, structural clustering and other template features. The quality and functionality of the obtained models were assessed using

the SWISS-MODEL server, and tertiary structures were validated through cross-validation. The phi-psi angles of amino acid residues in the structures of the three target proteins were analyzed using the Ramachandran plot, and the quality of the models was evaluated with MolProbity version 4.4. The z-scores of the proteins were verified using the ProSAweb server (Wiederstein et al., 2007).

2.4 Molecular docking

Molecular docking is an in silico, target-based computational biology analysis that examines the alignment and orientation of molecules at binding sites on protein targets. Predicting molecular interactions is a preliminary step in determining potential drug behaviors towards the target. Molecular docking was performed using the Autodock Vina v.12.5 with UCSF Chimera program (Pettersen et al., 2004). The CASTp 3.0 web server was used to identify protein binding sites, and molecular docking analysis was performed on the identified cavities (http://sts.bioe.uic.edu/castp). A grid box of 60x60x60 $Å^3$ was used for docking, and the Lamarckian Genetic Algorithm (LGA) was employed to explore the ligand-protein interactions. To validate the docking protocol, a re-docking procedure was performed by docking the co-crystallized ligands back into their respective binding sites of the target proteins. The Root Mean Square Deviation (RMSD) between the re-docked poses and the original crystal structures was calculated, with a threshold value of < 2.0 Å considered indicative of reliable docking accuracy. In our study, RMSD values of 0 Å were obtained, confirming the precision of the docking protocol. Also blind docking was performed using the receptor ligands provided by the PDB, following the same methodology as the study, to determine the threshold values of binding affinities for all three identified receptors and to compare these values with the data obtained from the study. After all docking analysis, 3D and 2D binding poses of the protein–ligand complexes were then analyzed and visualized by using the Discovery Studio Visualizer (Jejurikar et al., 2021). The inhibition constant (K_i) was calculated using the formula provided below (Gaiya et al., 2024).

$$\Delta G = -RTlnK$$

ΔG = Binding affinities (kcal/mol)
K_i = Inhibition constant
$R = 1.987 \times 10^{-3}$ $kcalmol^{-1}K^{-1}$ (Gas constant)
T = 298.15 K (absolute temperature)

2.5 Molecular dynamics

Phytosterols with the highest binding affinity (from the molecular docking analysis) were selected for molecular dynamics (MD) simulation studies. The MD simulation was performed using the AMBER99SB force field with the BioBB-Wfs-based MD algorithm (Andrio et al., 2019). Proteins and complexes were solvated in octahedral boxes using the TIP3P model. All structures were neutralized by adding counterions at a concentration of 0.05 to ensure electrical neutrality. The system was then equilibrated for 1 ns under both NVT (constant volume and temperature) and NPT (constant pressure and temperature) conditions. During the NVT equilibration, the temperature was maintained at 300 K, and during NPT equilibration, the pressure was kept at 1.0 bar. Following equilibration, a 500 ps MD simulation was performed. The trajectory of the simulation was analyzed by calculating the RMSD, radius of gyration (Rg), and GROMACS energies to assess the stability and structural changes of the system over time.

2.6 ADMET properties

Absorption, distribution, metabolism, excretion and toxicity (ADMET) properties of the selected phytosterols were predicted using the pkCSM (https://biosig.lab.uq.edu.au/pkcsm) and Swiss-ADME (http://www.swissadme.ch) web tools while drug-like properties were evaluated using the AI Drug-Lab (Tian et al., 2022). The ADMET predictions were interpreted by analyzing key molecular descriptors, pharmacokinetic properties and literature data. Molecular weight was assessed to ensure the compounds fall within the drug-like range, while hydrogen bond donors/acceptors and TPSA values were used to predict oral bioavailability and membrane permeability. Water solubility and lipophilicity (logP) were analyzed to determine the compounds' absorption and distribution characteristics. The number of rotatable bonds (ROTB) was evaluated as an indicator of molecular flexibility. Finally, Lipinski's rule violations were used to identify compounds that may have poor pharmacokinetic properties, providing an overall assessment of drug-likeness.

2.7. Statistical analysis

The statistical analysis was performed using Python 3 programming language. Binding energy data was processed using the Pandas library. A one-way ANOVA test was applied for significance testing, and this test was conducted using the SciPy library. The obtained p-value was used to determine whether the differences between groups were statistically significant, with significance accepted at $p < 0.05$.

Results

3.1 3D structure configuration prediction and validation

As shown in Figures 2A, 3A, and 4A, the 3D structural predictions of monkeypox A42R Profilin-like Protein (PDB ID: 4QWO), Methyltransferase VP39 (PDB ID: 8CEQ), and Phosphatase (PDB ID: 8GZ4) were obtained using the SWISS-MODEL server. Subsequently, structural assessments were performed, revealing Ramachandran plots with 97.71% residues in the most favored regions for 4QWO, 97.96% for 8CEQ, and 93.45% for 8GZ4 (Figures 2B, 3B, and 4B). During model refinement using the GalaxyWeb web-tool, the best model was chosen based on parameters including GDT-HA (0.9989), RMSD (0.184), MolProbity (1.16), clash score (8.03), poor rotamers (0.25%), and Ramachandran plot (97.71%) for 4QWO; GDT-HA (0.9998), RMSD (0.182), MolProbity (1.03), clash score (7.31), poor rotamers (0.73%), and Ramachan-

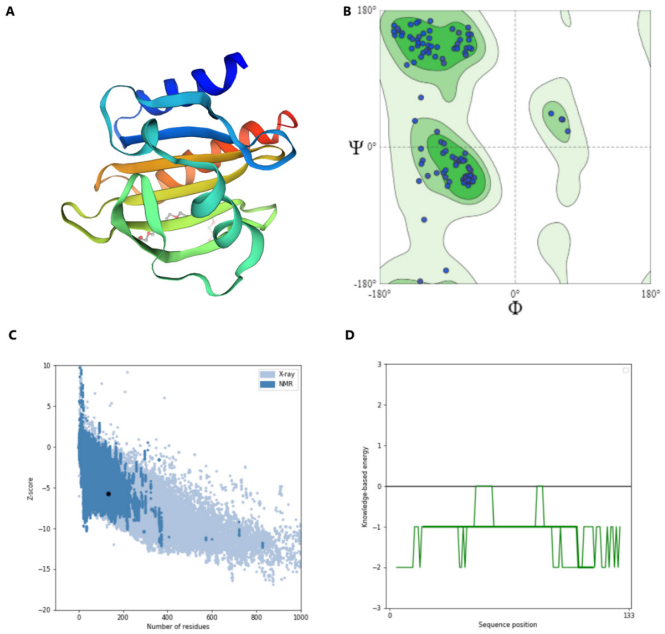

Figure 2. A42R Profilin-like Protein (PDB ID: 4QWO) from monkeypox, **A** Predicted 3D structure **B** Ramachandran plot (97.71%) residues in favored region, **C** Z-score graph NMR spectroscopy (dark blue) and X-ray crystallography (light blue), **D** ProSAweb server energy plot

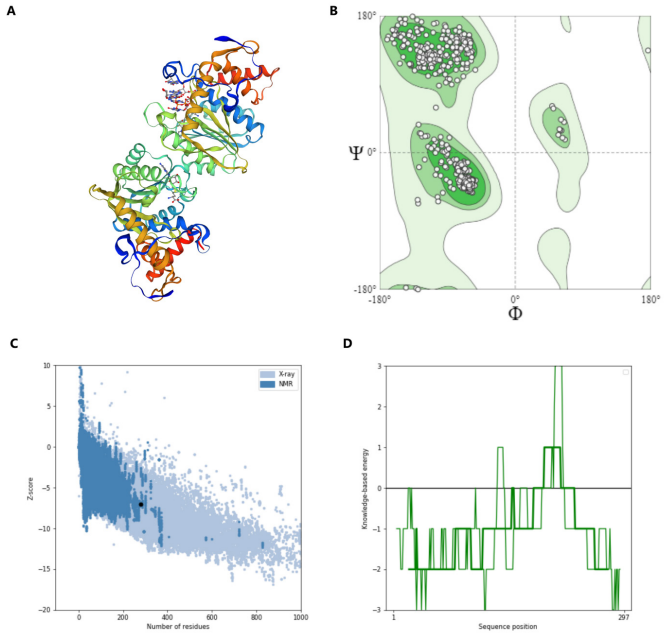

Figure 3. Methyltransferase VP39 (PDB ID: 8CEQ) from monkeypox, **A** Predicted 3D structure **B** Ramachandran plot (97.96%) residues in favored region, **C** Z-score graph NMR spectroscopy (dark blue) and X-ray crystallography (light blue), **D** ProSAweb server energy plot

dran plot (97.96%) for 8CEQ; and GDT-HA (0.9839), RMSD (0.261), MolProbity (1.16), clash score (2.09), poor rotamers (0.00%), and Ramachandran plot (93.45%) for 8GZ4. Additionally, ProSAweb analysis of monkeypox A42R Profilin-like Protein (PDB ID: 4QWO), Methyltransferase VP39 (PDB ID: 8CEQ), and Phosphatase (PDB ID: 8GZ4) yielded z-scores of -5.76, -7.06, and -7.96, respectively, indicating their placement within the range of native proteins (Figures 2C, 3C, and 4C). The results of the basic energy profile analysis are presented in Figures 2D, 3D, and 4D. The horizontal axis represents positions along the protein sequence, while the vertical axis shows knowledge-based energy values for each position. Negative energy values indicate that these regions of the protein structure are likely more stable and are frequently observed in native

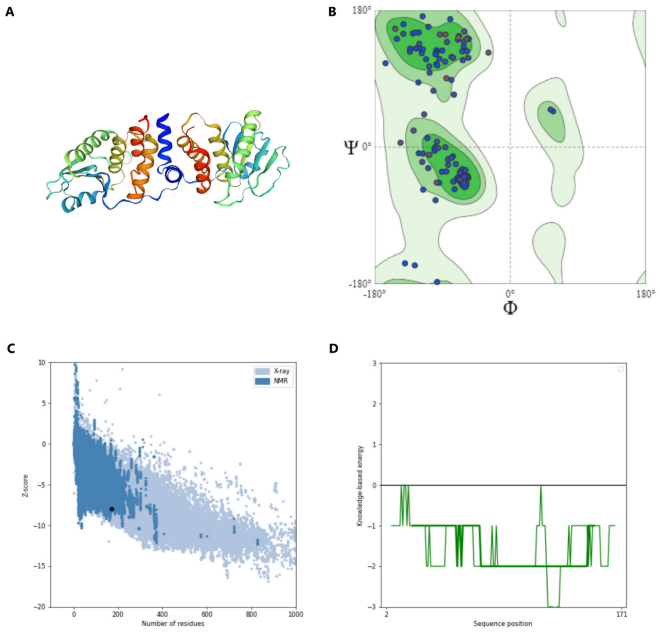

Figure 4. Phosphatase (PDB ID: 8GZ4) from monkeypox, **A** Predicted 3D structure **B** Ramachandran plot (93.45 %) residues in favored region, **C** Z-score graph NMR spectroscopy (dark blue) and X-ray crystallography (light blue), **D** ProSAweb server energy plot

protein structures, whereas positive energy values suggest regions of reduced stability. For all proteins, the results show concentrated negative energy values between -1 and -3, indicating that the protein structures are relatively stable. However, for the 8CEQ model, there is a notable increase in positive energy values between positions 100 and 200, peaking at around position 180 with a value of +3, suggesting instability in this part of the protein, which may indicate structural instability.

3.2 Molecular docking

Based on the results of molecular docking analysis, the six examined phytosterols and the positive control molecules exhibited negative binding affinities with the target monkeypox proteins. The structural conformations of the two phytosterols with the lowest binding affinities and the positive controls for each protein target, as derived from Tables 1, 2, and 3, are presented in Figures 5, 6, and 7. The binding affinities, docking sites, interacting amino acid residues and inhibition constant (Ki) values in μM for the interactions between monkeypox proteins and the phytosterols are detailed in Tables 1, 2, and 3. Additionally, the statistical evaluation results, which include a comparison of the results obtained from molecular docking analyses with the control groups, are presented in Table 4. Among the tested compounds, all phytosterols demonstrated moderate to high binding affinities across the three monkeypox protein targets—A42R Profilin-like Protein (PDB ID: 4QWO), Methyltransferase VP39 (PDB ID: 8CEQ), and Phosphatase (PDB ID: 8GZ4). Notably, all ligands were found to occupy cavities with identical volumes (1821 $Å^3$), suggesting a conserved binding pocket architecture across target proteins. According to the results obtained, Ergosterol peroxide exhibited the highest binding affinity of -8.1 kcal/mol for monkeypox's A42R Profilin-like Protein, 10-α-ergosterol and β-ergosterol showed an affinity of -8.9 kcal/mol for Methyltransferase VP39, and Ergosterol exhibited a score of -8.1 kcal/mol for Phosphatase. In terms of inhibitory potential, 10-α-ergosterol and β-ergosterol yielded Ki values of 0.29 μM for VP39, closely approaching the potency of Tecovirimat (0.21 μM), the positive control. Similarly, Ergosterol displayed a Ki of 1.15 μM against Phosphatase, outperforming both Tecovirimat (6.23 μM) and Cidofovir (24.07 μM). Key interaction residues such as LEU154, ALA158, PHE188, ASN161, and LYS186 were consistently involved in both phytosterol and Tecovirimat interactions with VP39, highlighting the potential of these sterols to mimic native ligand binding modes. Likewise, in the Phosphatase active site, recurring interactions with TYR140, TYR137, and LYS128 were observed for both Ergosterol and Tecovirimat, supporting their structural compatibility within the binding pocket. When site-specific binding studies were examined, Ergosterol's binding to Phosphatase prominently involves hydrogen bonding and hydrophobic interactions with key residues TYR140, TYR137, and LYS128, reflecting a stable and specific ligand-protein engagement. Likewise, 10-α-ergosterol and β-ergosterol form significant contacts with residues LEU154, ALA158, PHE188, ASN161, and LYS186 within the VP39 methyltransferase active site, closely resembling the interaction network of the antiviral drug Tecovirimat. In Figure 5-C, the first notable aspect of ergosterol peroxide-receptor binding is the side chain containing alkyl groups outside the cyclopentano-perhydrophenanthrene ring, which forms alkyl bonds with the receptor. The formation of these bonds, when compared to the control groups, suggests that the molecular functionality of the ergosterol peroxide structure is derived from its side chain (Merdivan et al., 2017). On the other hand, when examining the same active site

Table 1. Binding Affinities (ΔG), ligand interaction with amino acid residues and inhibition constant of phytosterols against A42R Profilin-like Protein from monkeypox (PDB ID: 4QWO)

Ligand	Binding affinities (ΔG) kcal/mol	Cavity volume ($Å^3$)	Interaction Residues	Inhibition constant (Ki) μM
Tecovirimat[a]	-8.8± 0.1	349	Conventional H bond: ARG119, THR120, ARG127, ARG129 Carbon H bond: ASP116 Pi- Alkyl interaction: HIS100 Amide- pi stacked: ARG119 Halogen: ASN78 Van der Waals: ASP10, LYS16, PHE17, TYR80, ARG115, ARG122, ASP123, ALA130	0.35
Cidofovir[b]	-6.6± 0.3	349	Conventional H bond: THR120, ARG127 Carbon H bond: ASN78 Pi-anion interaction: ASP116, ASP123 Van der Waals: ASN14, LYS16, PHE17, GLU77, TYR80, ARG115, ARG119, ARG122, ARG129	14.5
Ergosterol	-7.0± 0.0	349	Alkyl interaction: LYS6 Van der Waals: GLU9, ASP10, LYS13, GLU77, ASN78, TYR80, ARG122, HIS124, ARG127, ARG129, ALA130	7.38
α-Dihydroergosterol	-7.2± 0.6	349	Alkyl interaction: ALA130 Unfavorable donor-donor: ARG119 Van der Waals: ASN78, TYR80, HIS100, ASP116, THR120, ARG122, ASP123, ARG127, ARG129	5.26
β-ergosterol	-7.6± 1.2	349	Alkyl interaction: ILE7, ARG127 Van der Waals: ALA2, GLU3, LYS6, ASP10, GLU77, ASN78, TYR80, HIS100, HIS124, VAL128, ARG129, ALA130, THR131	2.68
Ergosterol peroxide	-8.1± 0.8	349	Conventional H bond: GLU77 Alkyl interaction: ARG127, VAL128, ALA130 Van der Waals: ALA2, LYS6, ILE7, ASP10, ASN78, TYR80, HIS100, HIS124, ARG129, THR131	1.15
9-α,10-β-methyl ergosterol	-7.6± 1.4	349	Alkyl interaction: ARG119, TYR118 Van der Waals: THR71, SER73, THR79, GLU83, ARG114, ARG115, TYR118, ARG119, ARG122	2.68
10-α-ergosterol	-7.7± 0.4	349	Alkyl interaction: LYS6, ILE7, ARG129, ALA130 Van der Waals: ALA2, GLU3, ASP10, GLU77, ASN78, TYR80, HIS100, ASP123, HIS124, THR126, ARG127, VAL128, THR131	2.26

'a and b' are positive controls

Table 2. Binding Affinities (ΔG), ligand interaction with amino acid residues and inhibition constant of phytosterols against methyltransferase VP39 from monkeypox (PDB ID: 8CEQ)

Ligand	Binding affinities (ΔG) kcal/mol	Cavity volume (Å^3)	Interaction Residues	Inhibition constant (Ki) μM
Tecovirimat[a]	-9.1± 0.0	1821	Conventional H bond: ASN161 Carbon H bond: ALA158 Pi- Alkyl interaction: LEU154, LEU221 Alkyl interaction: ARG97, ALA158 Van der Waals: HIS98, GLY96, PHE115, LYS186, TYR189, PHE188, ARG220	0.21
Cidofovir[b]	-7.1± 0.1	1821	Conventional H bond: GLY96, ASN161, LYS186 Carbon H bond: SER141 Pi-alkyl interaction: LEU154, ALA158 Amide-pi stacked: TYR157 Van der Waals: ARG97, ARG114, PHE115	6.23
Ergosterol	-8.3± 0.1	1821	Conventional H bond: ASN161 Pi-alkyl interaction: LEU154, ALA158, PHE188 Van der Waals: GLY96, ARG97, PHE115, ARG140, SER141, LEU154, TYR157, ASN161, LYS186, PHE188, LEU221	0.82
α-Dihydroergosterol	-8.0± 0.2	1821	Pi-alkyl interaction: ALA158, TYR189 Unfavorable donor-donor: ARG119 Van der Waals: ASN78, TYR80, HIS100, ASP116, THR120, ARG122, ASP123, ARG127, ARG129	1.36
β-ergosterol	-8.9± 0.3	1821	Pi-alkyl interaction: LEU154, ALA158, PHE188 Van der Waals: GLY96, ARG97, PHE115, SER141, TYR157, ASN161, LYS186, LEU221	0.29
Ergosterol peroxide	-8.2± 1.3	1821	Carbon H bond: ARG97 Alkyl interaction: ALA158 Pi-sigma interaction: TYR189 Van der Waals: GLY96, PHE115, LEU154, ASN161	0.97
9-α,10-β-methyl ergosterol	-8.4± 0.8	1821	Conventional H bond: LEU154 Alkyl interaction: ARG97, ALA158 Pi-alkyl interaction: TYR189, LEU221 Van der Waals: GLY96, PHE115, ASN161, LYS186, PHE188, ARG220	0.69
10-α-ergosterol	-8.9± 0.0	1821	Alkyl interaction: PHE115, ALA158, PHE188 Pi-alkyl interaction: LEU154, LEU221, LYS186 Van der Waals: GLY96, ARG97, HIS98, ASN161, SER165, PHE188, TYR189, MET219, ARG220	0.29

'a and b' are positive controls

Table 3. Binding Affinities (ΔG), ligand interaction with amino acid residues and inhibition constant of phytosterols against phosphatase from monkeypox (PDB ID: 8GZ4)

Ligand	Binding affinities (ΔG) kcal/mol	Cavity volume (Å^3)	Interaction Residues	Inhibition constant (Ki) μM
Tecovirimat[a]	-7.1 ± 0.2	1821	Pi- Alkyl interaction: TYR140 Pi-pi T shaped: TYR137 Alkyl interaction: LYS128 Van der Waals: THR31, ASN32, ASP100, TYR124, LEU125, SER132	6.23
Cidofovir[b]	-6.3 ± 1.0	1821	Conventional H bond: ASP100, ASN129, LYS130, TYR137 Pi-alkyl interaction: LYS128 Attractive charge: GLU131 Van der Waals: ASN32, SER132	24.07
Ergosterol	-8.1 ± 0.8	1821	Pi-sigma interaction: TYR140 Pi-alkyl interaction: LEU6, LEU136 Alkyl interaction: TYR9 Van der Waals: SER5, ARG13, HIS19, SER132, TYR137, ASP147	1.15
α-Dihydroergosterol	-7.3 ± 0.0	1821	Conventional H bond: ASP100 Pi-sigma interaction: TYR140 Pi-alkyl interaction: LEU6, LYS128, LEU136, TYR137 Van der Waals: THR31, ASN32, TYR124	4.45
β-ergosterol	-7.0 ± 0.3	1821	Pi-alkyl interaction: LYS128, TYR137, TYR140 Van der Waals: ASP100, TYR124, LEU136	7.38
Ergosterol peroxide	-7.4 ± 0.1	1821	Pi-sigma interaction: TYR140 Pi-alkyl interaction: LYS128, TYR137 Van der Waals: LEU6, THR31, ASP100, TYR124, LEU125, SER132, LEU136	3.75
9-α,10-β-methyl ergosterol	-7.9 ± 0.6	1821	Alkyl interaction: TYR9 Pi-alkyl interaction: LEU6, TYR140 Van der Waals: ASP2, SER5, ARG13, HIS19, TYR137, ASP147	1.61
10-α-ergosterol	-7.3 ± 0.0	1821	Alkyl interaction: LYS128 Pi-alkyl interaction: TYR137, TYR140 Van der Waals: LEU6, THR31, SER132	4.45

'a and b' are positive controls

Table 4. Statistical comparison of binding affinities across groups

Source of variation	Sum of Squares (SS)	Degrees of Freedom (df)	Mean Square (MS)	F-Statistic	p-value
Between groups	7.441860	2	9.302326	4.881356	0.069202
Within Groups	1.528571	5	0.305714	-	-
Total	2.445714	7	-	-	-

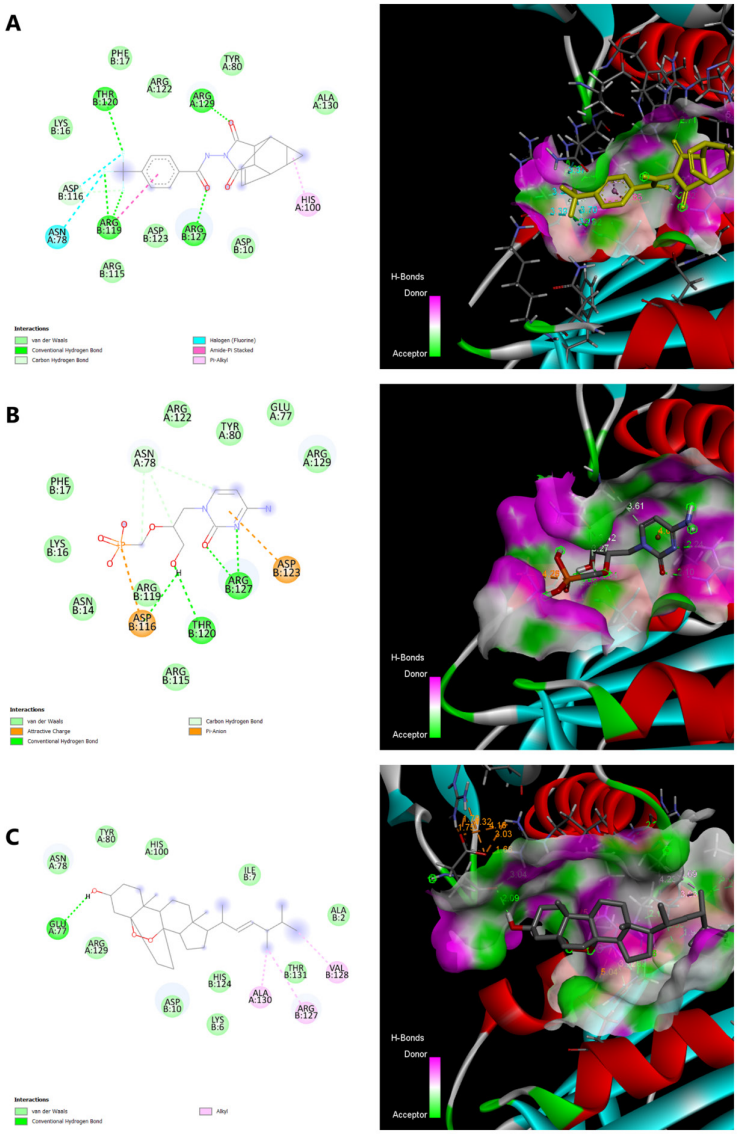

Figure 5. Two dimensional (2D) and three dimensional (3D) pose views of molecular docking interactions between A42R Profilin-like Protein (PDB ID: 4QWO) and **A** Tecovirimat, **B** Cidofovir (positive controls) and **C** Ergosterol peroxide

in Figure 6-C, the inwardly twisted chain structure attached to the C-17 atom of β-ergosterol, which maintains conformational stability, attempts to minimize the molecule's internal energy, resulting in a lower binding affinity compared to ergosterol peroxide (Giroux et al., 2008). A different binding behavior was observed for ergosterol, where the cyclopentano-perhydrophenanthrene part was determined to be more active and binding-preferable (Figure 7-C). It is thought that this is due to the strategic positioning of the double bonds, which allow ergosterol to evolve in a flexible and biotransformable manner. Due to the presence of the peroxide group, ergosterol peroxide is a more polar molecule, and since molecular docking interactions are primarily based on polarity and hydrophobicity, this structural difference is believed to influence the binding and scoring (Yang et al., 2015). On the other hand, as a result of the ANOVA analyses performed to compare the binding affinities obtained from the docking analyses, it was found that there is no significant difference between the phytosterol scores and the control group (Tecovirimat and Cidofovir) (Table 4). The p-value (0.069) indicates that this difference is not statistically significant and suggests that the binding affinities of the phytosterols are similar to those of the control group.

3.3 Molecular dynamics simulation

The molecular dynamic behaviors of β-ergosterol for Methyltransferase VP39 were analyzed. Figures 8 illustrate the root mean square deviations (RMSD) at 0 to 500 ps to examine the stable hydrogen bonds between the component and the protein target. The results of the analyses indicate that the number of H-bonds and the binding-free energy of interaction play a significant role in the stabilization of the complex and the inhibitory interactions. The total energy of the protein-ligand complex from the GROMACS energies plot exhibited a significant

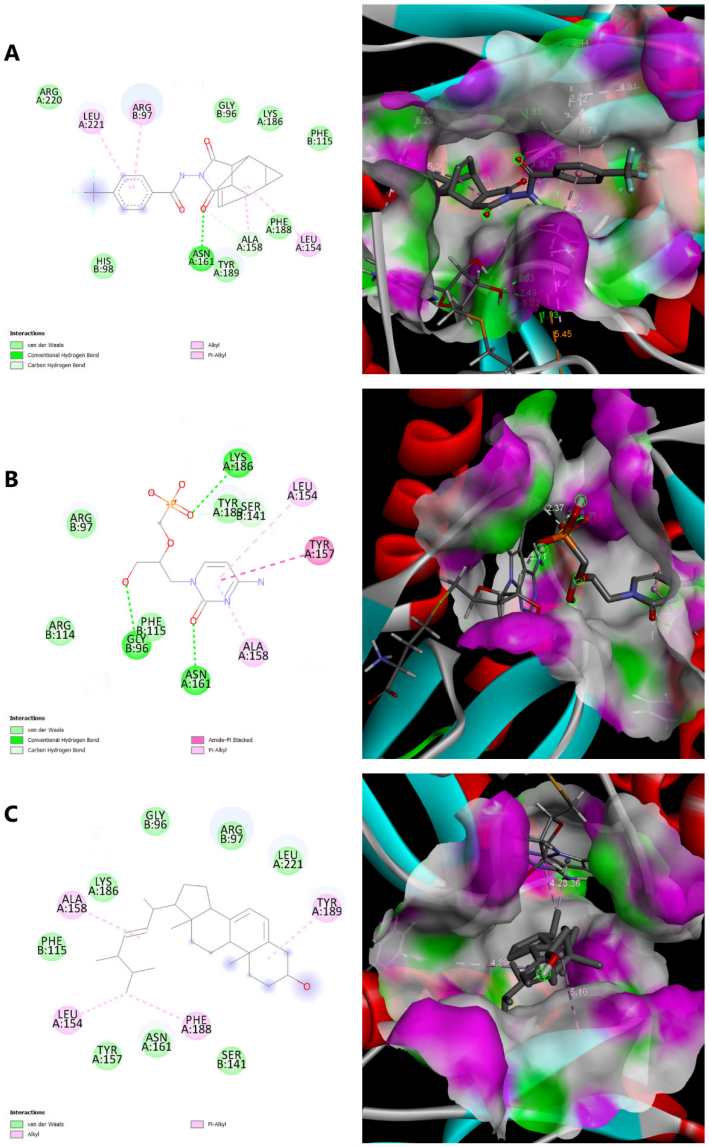

Figure 6. Two dimensional (2D) and three dimensional (3D) pose views of molecular docking interactions between Methyltransferase VP39 (PDB ID: 8CEQ) and **A** Tecovirimat, **B** Cidofovir (positive controls) and **C** β-ergosterol

binding free energy compared to the potential energy which corroborate with the report of the Kaur et al. 2023.

3.4 Assessment of ADMET properties

The ADMET properties of ergosterol and its derivative phytosterols were assessed to determine their drug-like characteristics and to evaluate their physicochemical and pharmacokinetic profiles. None of the compounds violated Lipinski's Rule of Five but phytosterols slightly exceed the molecular weight limit (Table 5). From Table 5, all the phytosterols exhibit favorable hydrogen bond donor/acceptor ratios (1/1 or 1/3) and moderate solubility characteristics. Ergosterol peroxide and the other ergosterol derivatives are moderately soluble, while Tecovirimat and Cidofovir are highly soluble. In terms of lipophilicity (LogP), all compounds show logP values greater than 2, indicating moderate to high lipophilicity, with ergosterol derivatives showing slightly higher values (LogP ~4.6-4.9), which indicate better cell membrane permeability. The total polar surface area (TPSA) values for the compounds range from 20.23 to 157.71 Å^2, with Cidofovir having the highest TPSA (157.71 Å^2), indicating a greater potential for hydrogen bonding and possible difficulty in crossing lipid membranes compared to the phytosterols. The bioavailability score for all phytosterols was greater than zero, suggesting good bioavailability and efficient membrane permeability. None of the compounds demonstrated blood-brain barrier (BBB) permeability, which may reduce the risk of central nervous system side effects. In terms of metabolic interactions, the phytosterols and positive control compounds were evaluated for their interactions with critical drug-metabolizing enzymes (CYP3A4 and CYP2D6). While the phytosterols showed some degree of inhibition of these enzymes, they remained within safe limits for drug metabolism interactions (Table 6). Regarding clearance, ergosterol peroxide showed the fastest absorption, while ergosterol exhibited

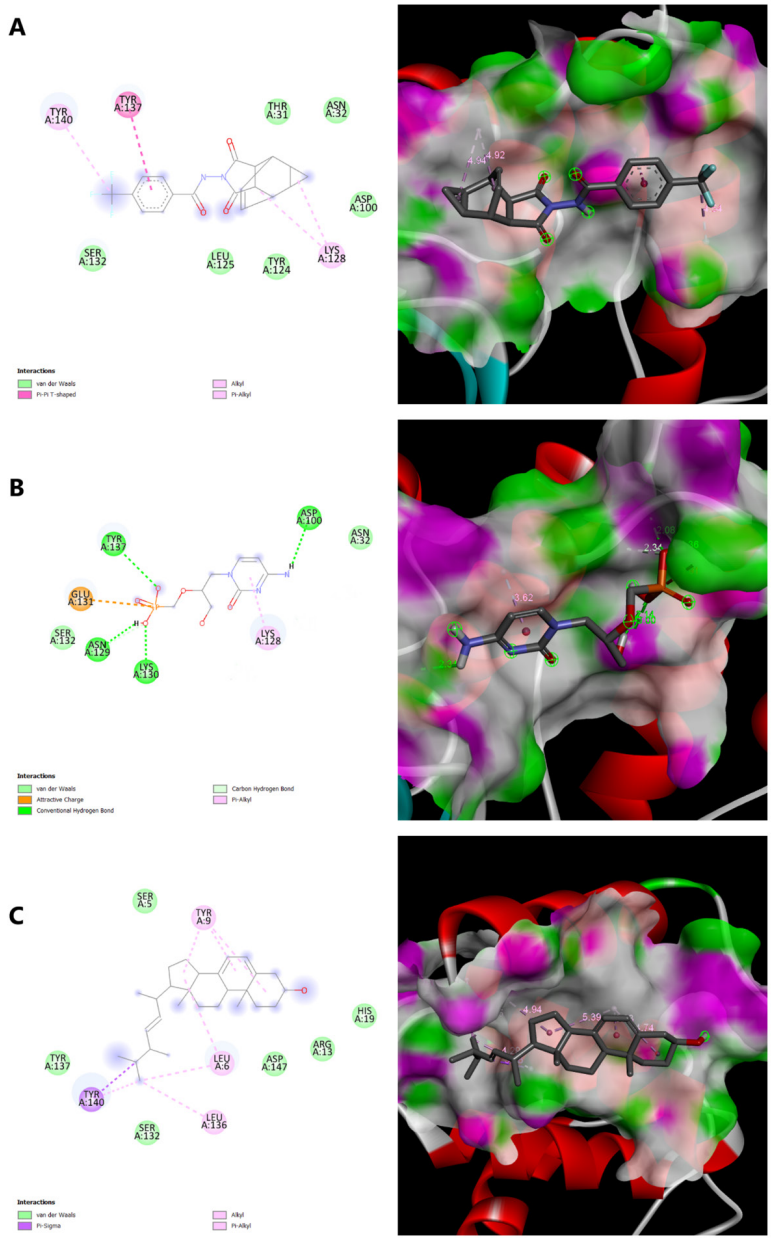

Figure 7. Two dimensional (2D) and three dimensional (3D) pose views of molecular docking interactions between Phosphatase (PDB ID: 8GZ4) and **A** Tecovirimat, **B** Cidofovir (positive controls) and **C** Ergosterol

the slowest absorption. HLM stability is an in vitro assay that measures how rapidly a compound is metabolized by enzymes present in human liver microsomes. This test provides insights into the metabolic degradation rate of a drug in the liver, thereby contributing to the prediction of its bioavailability and pharmacokinetic profile (Lee et al., 2007). Upon analysis of the data, it appears that ergosterol and its derivatives may exhibit high metabolic stability in human liver microsomes. This suggests that these compounds are metabolized slowly in the liver, allowing them to persist longer in the system, which may confer a pharmacokinetic advantage. Among the reference antiviral agents, Tecovirimat showed low stability, indicating rapid hepatic metabolism, while Cidofovir demonstrated moderate stability. In this context, based on in silico evaluation, ergosterol derivatives are considered to potentially exhibit a superior metabolic stability profile compared to both Tecovirimat and Cidofovir. When compared to the positive controls, the phytosterols did not show any significant toxicity, further supporting their potential as safe therapeutic agents (Table 7).

Discussion

Mushrooms, with their powerful bioactive components, are not only a common part of nature but also potential sources of therapeutic agents that have caught the attention of modern medicine (Lysakowska et al., 2023). Additionally, they serve as

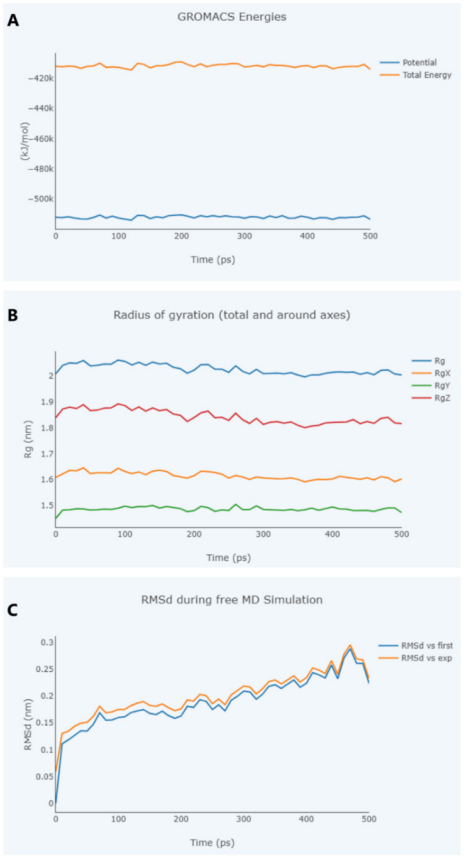

Figure 8. Molecular dynamics simulation of Methyltransferase VP39 (PDB: 8CEQ) and β-ergosterol. **A** GROMACS Energies **B** Radius of gyration **C** RMSD

Table 5. Physicochemical properties and Lipinski's rule of five for drug-likeness analysis of ergosterol and derivative phytosterols

Ligand	Molecular weight (g/mol)	Hydrogen bond donors/acceptors	Water Solubility	Lipophilicity (logP)	TPSA (Å^2)	ROTB	Lipinski's rule violations
Tecovirimat	376.33	1/6	Soluble	2.28	66.48	4	0
Cidofovir	279.19	4/7	Soluble	-0.13	157.71	6	0
Ergosterol	396.65	1/1	Moderately soluble	4.92	20.23	4	1
α-Dihydroergosterol	398.66	1/1	Moderately soluble	4.77	20.23	4	1
β-ergosterol	396.65	1/1	Moderately soluble	4.92	20.23	4	1
Ergosterol peroxide	428.65	1/3	Moderately soluble	4.64	38.69	4	1
9-α,10-β-methyl ergosterol	396.65	1/1	Moderately soluble	4.77	20.23	4	1
10-α-ergosterol	396.65	1/1	Moderately soluble	4.92	20.23	4	1

TPSA as topological polar surface area and ROTB as number of rotatable bonds

Table 6. Pharmacokinetics of ergosterol and derivative phytosterols

Ligand	Human Intestinal Absorption	BBB permeability	Skin permeability	Bioavailability Score	P-gp substrate	Clearence	CYP3A4 inhibitor	CYP2D6 inhibitor	HLM Stability
Tecovirimat	Absorbed	No	-3.19	0.55	No	9.05	Yes	No	Poor
Cidofovir	Absorbed	No	-2.76	0.11	No	2.44	No	No	Moderate
Ergosterol	Absorbed	No	-2.83	0.55	No	5.22	No	No	High
α-Dihydroergosterol	Absorbed	No	-2.80	0.55	No	7.87	No	No	High
β-ergosterol	Absorbed	No	-2.83	0.55	No	5.22	No	No	High
Ergosterol peroxide	Absorbed	No	-2.47	0.55	No	12.20	No	No	High
9-α,10-β-methyl ergosterol	Absorbed	No	-2.84	0.55	No	5.43	No	No	High
10-α-ergosterol	Absorbed	No	-2.80	0.55	No	5.89	No	No	High

Blood–brain barrier (BBB) permeability and P-glycoprotein (P-gp)

Table 7. Toxicity profile of ergosterol and derivative phytosterols

Ligand	Hepatotoxicity	Carcinogenicity	Ames mutagenesis	Nephrotoxicity	Biodegradation
Tecovirimat	Safe	Safe	Safe	Safe	Safe
Cidofovir	Moderately safe	Toxic	Moderately safe	Moderately safe	Safe
Ergosterol	Safe	Safe	Safe	Safe	Safe
α-Dihydroergosterol	Safe	Safe	Safe	Safe	Safe
β-ergosterol	Moderately safe	Safe	Moderately safe	Moderately safe	Safe
Ergosterol peroxide	Safe	Safe	Safe	Safe	Safe
9-α,10-β-methyl ergosterol	Moderately safe	Safe	Moderately safe	Moderately safe	Safe
10-α-ergosterol	Moderately safe	Safe	Moderately safe	Moderately safe	Safe

essential "functional" food sources in culinary applications (Adetunji et al., 2022). Mushrooms contain a rich array of bioactive substances such as polysaccharides, sterols, proteins, vitamins (especially B and D), minerals, and phenolic compounds (Arshadi et al., 2023). Examples like shiitake, maitake, reishi, portobello, cordyceps, and chaga mushrooms are notable for their dual role in edible and medicinal uses, providing a wealth of bioactive content (Phillips et al., 2022). In this study, ergosterol and its derivatives were selected as ligands based on several key criteria. Ergosterol is an important fungal sterol that contributes to cell membrane integrity and exhibits unique structural features, making it an excellent candidate for bioactivity screening. Previous studies have demonstrated the critical role of ergosterol derivatives in combating viral infections with focusing mainly on inflammation markers has highlighted their high antiviral effects against various viruses, including Influenza A (Zhou et al., 2019), porcine delta-coronavirus (Duan et al., 2021), and Hepatitis D (Chiou et al., 2024). Moreover, ergosterol can be sustainably sourced from fungal biomass, including waste products from mushroom cultivation, making it an environmentally friendly and cost-effective therapeutic resource (Gessner 2020). Molecular docking is one of the most used techniques in drug discovery to structurally analyze molecules believed to have therapeutic activity against a receptor target. By studying the interaction of amino acid residues in the active pockets of receptor proteins, this technique contributes to the disease-specific investigation of potential biotherapeutic molecules and serves as an important preliminary step for in vitro and in vivo studies (Sahu et al., 2024). The evaluation of natural molecules with antiviral potential has reached its peak

during the SARS-CoV-2 pandemic, as the demand for drug discovery has increased (Dilip 2024). This process, which accelerates the discovery of inhibitory activity and serves as a precursor to experimental procedures, has also contributed to the recognition and validation of in silico analyses. As of August 2024, following the declaration by the WHO Director-General that the monkeypox outbreak is a public health emergency of international concern, the investigation and development of biotherapeutic products for managing viral diseases have remained a significant topic (El-Dine et al., 2024). So, the analyses conducted in this study focus on exploring how ergosterol and its derivatives, abundant in mushroom species like *Agaricus bisporus, Lentinula edodes*, and *Pleurotus ostreatus*, exhibit inhibitory effects against monkeypox. The results obtained from molecular docking studies demonstrate that the tested phytosterol ligands displayed strong binding affinities with the target protein structures, surpassing the binding affinities of the positive control drugs Tecovirimat and Cidofovir, with negative binding scores. The interaction between β-ergosterol and the methyltransferase VP39 target protein, which achieved the highest binding score of -8.9 kcal/mol, can be attributed to significant Pi-alkyl interactions. The binding of amino acid residues in the target protein to the ring structures of the ligands also contributed to the increased binding score and inhibitory activity. Methyltransferase inhibition has been proposed as an antiviral strategy in studies conducted on various virus types (Song et al., 2021). The strong interaction demonstrated by β-ergosterol with monkeypox's methyltransferase suggests that mushrooms containing β-ergosterol, such as *Ganoderma lucidum* or *Ganoderma sichuanense*, may serve as potential biotherapeutic agents in combating the disease (Vazirian et al., 2014). Notably, in the inhibitor design study published for the discovery of the 3D structure of methyltransferase VP39 (8CEQ), it was determined that nearly all ligands interacted with the amino acid residues ARG97, PHE115, and ASN158 (Silhan et al., 2023). As a result of the molecular docking analysis conducted to determine the threshold binding affinities for the receptors, the following binding affinity values were obtained: for methyltransferase VP39 (Ligand Pubchem ID: 167530895), -9.5 kcal/mol; for A42R Profilin-like Protein (Ligand Pubchem ID: 8117), -4.0 kcal/mol; and for phosphatase (Ligand Pubchem ID: 1061), -6.7 kcal/mol. When compared to the threshold values of phytosterol binding affinities ranging from -8.1 to -7 kcal/mol obtained in this study, it can be stated that for A42R Profilin-like Protein and phosphatase bindings, phytosterols exhibited better docking behaviors than the receptor-specific ligands. Research studies evaluating the antiviral effects of phytosterols through in silico methods predominantly focus on receptor proteins involved in synthase activity or protein structures facilitating infectivity. Shokry et al. evaluated the antiviral effects of β-Sitosterol, a phytosterol, on the Influenza A Virus through in silico methods and reported that the binding scores of various viral protein structures ranged between -5 and -30 kcal/mol (Shokry et al., 2023). Similarly, in another study conducted on phytosterols, their effects on SARS-CoV-2 were evaluated in silico, with the main protease selected as the receptor. The highest binding score was reported for Stigmasterol glucoside at -8.2 kcal/mol (Rahmatullah et al., 2021). After the molecular docking analysis, the highest-scoring component was subsequently subjected to MD analysis. Molecular docking analyses typically rely on static, single conformations, which do not fully capture the dynamic and flexible nature of biological systems. To address this limitation, MD simulations were employed to evaluate the temporal behavior, conformational changes, and stability of protein-ligand interactions. Within this study, MD simulations served as a complementary method to validate and enhance the biological relevance of docking results by reflecting the functional dynamics of protein-ligand complexes associated with maximum inhibitory activity (Kato et al., 2021). The results from MD analysis (Figure 8A), when examined in terms of the GROMACS energy output, indicate that the blue line representing potential energy remained stable throughout the simulation, with minor fluctuations and no major changes (Lee et al., 2016). This suggests that the system was energetically stable, with balanced dynamics. This stability implies that the molecules remained at a steady point on the potential energy surface, with no major structural alterations during the simulation. Similarly, the total energy, represented by the orange line, remained consistent. Since total energy includes both kinetic and potential energy, a trend similar to potential energy was expected. It was determined that the system remained balanced and stable throughout the simulation. The Rg (radius of gyration) value, depicted in Figure 8B, is an important parameter used to assess structural properties such as shape, size, and flexibility of a molecule. It is particularly employed in molecular dynamics simulations of proteins, polymers, or other large biomolecules (Yamamoto et al., 2021). The overall Rg value fluctuated around 2.0 nm, with only slight variations over time. This indicates that the molecule retained its general structural stability and did not undergo dramatic conformational changes such as collapse or expansion. Throughout the simulation, the protein remained in a stable state without significant deformation. However, the radius of gyration along the Z-axis (RgZ) varied between 1.8 and 1.9 nm over time. This suggests that the protein's asymmetric folding regions extended along the Z-axis. The RgY and RgX values, which hovered around 1.5 nm, reflected a more compact and stable behavior compared to other regions. These axis-specific behaviors indicate that the binding interactions between the protein and ligand were stabilized and remained compact throughout the simulation (Liu et al., 2017). When examining the ADMET properties, all the analyzed phytosterols exhibited profiles comparable to the positive control drugs, with good pharmacokinetic properties. The toxicity predictions, which were unsurprisingly low, suggest that mushroom ergosterols can be safely explored and used (Tevyashova et al., 2023). It appears that the investigated phytosterols share similar active binding regions and amino acid residues with drug molecules when targeting monkeypox receptor proteins. This indicates that ergosterol and its derivatives effectively interact with the

target receptors and could potentially be investigated for drug design purposes as potential inhibitors.

Conclusion

This study aimed to evaluate the in silico interactions of ergosterol and its derivative phytosterols with monkeypox protein targets and to explore their potential biotherapeutic efficacy. The results revealed that β-ergosterol exhibited methyltransferase VP39 inhibitor activity with a binding affinity score of -8.9 kcal/mol. Additionally, ergosterol peroxide was identified as the most effective ligand for the A42R Profilin-like Protein with a binding affinity of -8.1 kcal/mol, and ergosterol demonstrated the strongest interaction with phosphatase, also at -8.1 kcal/mol. Molecular interactions between ergosterol and its derivatives with monkeypox target proteins showed high inhibitory binding affinities ($\Delta G \geq 6.7$ kcal/mol). The results from MD simulations also confirmed that the β-ergosterol interactions remained stable under specific temperature, pressure, and water molecule conditions, exhibiting compact behavior around the optimal temperature of 300 K. Furthermore, in addition to β-ergosterol, the ergosterol and its derivatives analyzed in the study demonstrated excellent pharmacokinetic properties. These compounds were bioavailable, provided good human gastrointestinal absorption, were non-carcinogenic, non-AMES toxic, non-permeable to the BBB, non-inhibitory to CYP3A4 and CYP2D6 cytochrome P450 enzymes and not substrates for P-gp. Therefore, our findings are preliminary and suggest that ergosterol and its derivative phytosterols could be promising candidates against monkeypox. However, further experimental validation through controlled in vitro and in vivo testing is required before considering their therapeutic application.

Acknowledgements

The authors are thankful to UCSF Chimera team for allowing using programs for molecular visualization and molecular docking.

Author contributions

SK, NV and HTC designed the research and revised the manuscript. SK and NV performed virtual screening and bioinformatics analysis. All authors have read and approved the final manuscript.

Data availability

All data has been included inside the manuscript.

Declarations

The authors claim that the researchers in this study have no conflict of interest.

References

1. Adetunji CO, Olaniyan OT, Adetunji JB, Osemwegie OO, Ubi BE. African mushrooms as functional foods and nutraceuticals. Fermentation and Algal Biotechnologies for the Food, Beverage and Other Bioproduct Industries, Murdoch, Australia 2022
2. Andrade JC, Braga MFBM, Guedes GMM, Tintino SR, Freitas MA, Quintans LJ, Menezes IR, Coutinho HD. Cholecalciferol, ergosterol, and cholesterol enhance the antibiotic activity of drugs. International Journal for Vitamin and Nutrition Research 2019; 88(3):5-6.
3. Andrio P, Hospital A, Conejero J, Jordá L, Del-Pino M, Codo L, Soiland-Reyes S, Goble C, Lezzi D, Badia RM, Orozco M. BioExcel Building Blocks, a software library for interoperable biomolecular simulation workflows. Sci Data 2019; 6(1):169.
4. Arshadi N, Nouri H, Moghimi H. Increasing the production of the bioactive compounds in medicinal mushrooms: an omics perspective. Microb Cell Fact 2023; 22(1):11.
5. Bottini A, Pacheco DR, Forti FL, Bottini N. Revisiting VH1 phosphatase at the time of monkeypox: back to the spotlight. Biochem. Soc. Trans. 2023; 51(4): 1419-1427.
6. Baruah P, Patra A, Barge S, Khan MR, Mukherjee AK. Therapeutic potential of bioactive compounds from edible mushrooms to attenuate SARS-CoV-2 infection and some complications of coronavirus disease (COVID-19). JoF 2023; 9(9):897.
7. Brennan G, Stoian AM, Yu H, Rahman MJ, Banerjee S, Stroup JN, Park C, Tazi L, Rothenburg S. Molecular mechanisms of poxvirus evolution. MBio 2023; 14(1):22.
8. Bunge EM, Hoet B, Chen L, Lienert F, Weidenthaler H, Baer LR, Steffen R. The changing epidemiology of human monkeypox—A potential threat? A systematic review. PLoS Negl Trop Dis 2022; 16(2):141.
9. Burley SK, Berman HM, Kleywegt GJ, Markley JL, Nakamura H, Velankar S. Protein Data Bank (PDB): the single global macromolecular structure archive, Protein crystallography: methods and protocols, New York, USA. 2017
10. Chiou WC, Lyu YS, Hsia TL, Chen JC, Lin LC, Chang MF, Huang C. Ergosterol peroxide blocks HDV infection as a novel entry inhibitor by targeting human NTCP receptor. Biomed Pharmacother. 2024; (170): 116077.
11. Choy HL, Gaylord EA, Doering TL. Ergosterol distribution controls surface structure formation and fungal pathogenicity. Mbio 2023; 14(4):13.
12. Cui W, Huang H, Duan Y, Luo Z, Wang H, Zhang T, Nguyen HC, Shen W, Su D, Li X, Ji X. Crystal structure of monkeypox H1 phosphatase, an antiviral drug target. Protein & Cell 2023; 14(6):469
13. Daina A, Michielin O, Zoete V. SwissADME: a free web tool to evaluate pharmacokinetics, drug-likeness and medicinal chemistry friendliness of small molecules. Sci Rep 2017; 7(1):42.
14. Dilip-Bhandare S. Exploration of medicinal plants as potential therapeutics against COVID-19: molecular insights

and drug development prospects with other significant medicinal information. JPP 2024; rgae074.
15. Duan C, Ge X, Wang J, Wei Z, Feng WH, Wang J. Ergosterol peroxide exhibits antiviral and immunomodulatory abilities against porcine deltacoronavirus (PDCoV) via suppression of NF-κB and p38/MAPK signaling pathways in vitro. Int. Immunopharmacol.2021; (93): 107317
16. El-Dine FB, Gebreal A, Samhouri D, Estifanos H, Kourampi I, Abdelrhem H, Mostafa HAA, Elshaar AG, Suvvari TK, Ghazy RM. Ethical considerations during Mpox Outbreak: a scoping review. BMC Med Ethics 2024; 25(1):79.
17. Eng YS, Lee CH, Lee WC, Huang CC, Chang JS. Unraveling the molecular mechanism of traditional chinese medicine: formulas against acute airway viral infections as examples. Molecules 2019; 24(19):3505.
18. Farahat RA, Sah R, El-Sakka AA, Benmelouka AY, Kundu M, Labieb F, Shaheen RS, Abdelaal A, Abdelazeem B, Bonilla-Aldana DK, Franco-Paredes C. Human monkeypox disease (MPX). Le infezioni in Medicina 2022; 30(3):372.
19. Gaiya DD, Muhammad A, Musa JS, Auta R, Dadah AJ, Bello RO, Hassan M, Eke SS, Odihi RI, Sankey M. In silico analysis of balsaminol as anti-viral agents targeting SARS-CoV-2 main protease, spike receptor binding domain and papain-like protease receptors. In Silico Pharmacol 2024; 12(2):75.
20. Gessner MO. Ergosterol as a measure of fungal biomass. Methods to study litter decomposition: A practical guide 2020; 247-255.
21. Giroux S, Corey EJ. An efficient, stereocontrolled synthesis of the 25-(R)-diastereomer of dafachronic acid A from β-ergosterol. Org. Lett. 2008; 10(5): 801-802.
22. Hammann S, Lehnert K, Vetter W. Esterified sterols and their contribution to the total sterols in edible mushrooms. J Food Compos Anal 2016; 54:48-54.
23. Heo L, Park H, Seok C. GalaxyRefine: Protein structure refinement driven by side-chain repacking. NAR 2013; 41(1):384.
24. Hu D, Chen W, Li X, Yue T, Zhang Z, Feng Z, Li C, Bu X, Li QX, Hu CY, Li L. Ultraviolet irradiation increased the concentration of vitamin D2 and decreased the concentration of ergosterol in shiitake mushroom (Lentinus edodes) and oyster mushroom (Pleurotus ostreatus) powder in ethanol suspension. ACS omega 2020; 5(13):7361-7368.
25. Jejurikar BL, Rohane SH. Drug designing in discovery studio. AJRC 2021; 14(2):135.
26. Kato K, Nakayoshi T, Kurimoto E, Oda A. Molecular dynamics simulations for the protein–ligand complex structures obtained by computational docking studies using implicit or explicit solvents. Chem Phys Lett 2021; (781):139022
27. Kaur M, Sharma A, Kaur H, Singh M, Devi B, Naresh-Raj AR, Sood V, Pandey A, Gartia J, Kumar R, Suresh-Babu AR. Screening of potential inhibitors against structural proteins from Monkeypox and related viruses of Poxviridae family via docking and molecular dynamics simulation. J Biomol Struct Dyn 2023; 1-16.
28. Lee J, Cheng X, Jo S, MacKerell AD, Klauda JB, Im W. CHARMM-GUI input generator for NAMD, GROMACS, AMBER, OpenMM, and CHARMM/OpenMM simulations using the CHARMM36 additive force field. Biophys. J 2016; 110(3):641.
29. Lee PH, Cucurull-Sanchez L, Lu J, Du YJ. Development of in silico models for human liver microsomal stability. J Comput Aided Mol Des 2007; 21:665-673
30. Li Y, Zhao H, Wilkins K, Hughes C, Damon IK. Real-time PCR assays for the specific detection of monkeypox virus West African and Congo Basin strain DNA. J Virol Methods 2010; 169(1):223.
31. Liu P, Lu J, Yu H, Ren N, Lockwood FE, Wang QJ. Lubricant shear thinning behavior correlated with variation of radius of gyration via molecular dynamics simulations. J Chem Phys 2017; 147(8).
32. Łysakowska P, Sobota A, Wirkijowska A. Medicinal mushrooms: their bioactive components, nutritional value and application in functional food production—a review. Molecules 2023; 28(14):5393.
33. Martín-Delgado MC, Sánchez FJM, Martínez-Sellés M, García JMM, Guillén SM, Rodríguez-Artalejo F, Ruiz-Galiana J, Cantón R, Ramos PDL, García-Botella A, García-Lledó A. Monkeypox in humans: a new outbreak. Revista Española de Quimioterapia 2022; 35(6):509.
34. Merdivan S, Lindequist U. Ergosterol peroxide: a mushroom-derived compound with promising biological activities– a review. Int. J. Med. Mushrooms 2017; 19(2).
35. Minasov G, Inniss NL, Shuvalova L, Anderson WF, Satchell KJ. Structure of the Monkeypox virus profilin-like protein A42R reveals potential functional differences from cellular profilins. Struct. Biol. Cryst. Commun 2022; 78(10): 371-377.
36. Mitjà O, Ogoina D, Titanji BK, Galvan C, Muyembe JJ, Marks M, Orkin CM. Monkeypox. The Lancet, 2023; 401(10370):60.
37. Pettersen EF, Goddard TD, Huang CC, Couch GS, Greenblatt DM, Meng E, Ferrin TE. UCSF Chimera—a visualization system for exploratory research and analysis. J Comput Chem 2004; 25(13):1605.
38. Phillips JM, Ooi SL, Pak SC. Health-promoting properties of medicinal mushrooms and their bioactive compounds for the COVID-19 era—an appraisal: do the pro-health claims measure up?. Molecules 2022; 27(7):2302.
39. Rahmatullah M. (2021). In Silico Studies on the Binding of Phytosterols and Derivatives to SARS-CoV-2 Main Protease. ECPT 2021; (9):03-11
40. Rangsinth P, Sharika R, Pattarachotanant N, Duangjan C, Wongwan C, Sillapachaiyaporn C, Nilkhet S, Wongsirojkul N, Prasansuklab A, Tencomnao T, Leung GPH. Potential beneficial effects and pharmacological properties of ergosterol, a common bioactive compound in edible mushrooms. Foods 2023; 12(13):2529.
41. Rani I, Joshi H, Sharma U, Kaur J, Sood S, Ramniwas S,

Chauhan A, Abdulabbas HS, Tuli HS. Potential use of cidofovir, brincidofovir, and tecovirimat drugs in fighting monkeypox infection: recent trends and advancements. Naunyn Schmiedebergs Arch Pharmacol 2024; 397(4):2055.
42. Reynolds MG, Davidson WB, Curns AT, Conover CS, Huhn G, Davis JP, Wegner M, Croft DR, Newman A, Obiesie NN, Hansen GR. Spectrum of infection and risk factors for human monkeypox, United States, 2003. Emerg Infect Dis 2007; 13(9):1332.
43. Sahu A, Rathor LS, Dwivedi SD, Shah K, Chauhan NS, Singh MR, Singh D. A review on molecular docking as an interpretative tool for molecular targets in disease management. Assay and drug development technologies 2024; 22(1):40.
44. Saied AA, Dhawan M, Metwally AA, Fahrni ML, Choudhary P, Choudhary OP. Disease history, pathogenesis, diagnostics, and therapeutics for human monkeypox disease: a comprehensive review. Vaccines 2022; 10(12):2091.
45. Shokry S, Hegazy A, Abbas AM, Mostafa I, Eissa IH, Metwaly AM, Mostafa A. Phytoestrogen β-sitosterol exhibits potent in vitro antiviral activity against influenza a viruses. Vaccines 2023; 11(2): 228.
46. Silhan J, Klima M, Otava T, Skvara P, Chalupska D, Chalupsky K, Kozic J, Nencka R, Boura E. Discovery and structural characterization of monkeypox virus methyltransferase VP39 inhibitors reveal similarities to SARS-CoV-2 nsp14 methyltransferase. Nat Commun 2023; 14(1):2259.
47. Škvára P. Structural analysis of 2'-O-methyltransferase VP39 derived from mpox virus. Dissertation, Charles University, Prag, 2024.
48. Song W, Zhang H, Zhang Y, Chen Y, Lin Y, Han Y, Jiang J. Identification and characterization of Zika virus NS5 methyltransferase inhibitors. Front cell infect microbiol 2021; 11:665379.
49. Talwar S, Sood S, Kumar J, Chauhan R, Sharma M, Tuli HS (2020) Ayurveda and allopathic therapeutic strategies in coronavirus pandemic treatment. Curr Pharmacol Rep 2020; 6:354.
50. Taofiq O, Martins A, Barreiro MF, Ferreira IC. Anti-inflammatory potential of mushroom extracts and isolated metabolites. Trends Food Sci Technol 2016; 50:193.
51. Tevyashova A, Efimova S, Alexandrov A, Omelchuk O, Ghazy E, Bychkova E, Zatonsky G, Grammatikova N, Dezhenkova L, Solovieva S, Ostroumova O. Semisynthetic amides of amphotericin B and nystatin A1: A comparative study of in vitro activity/toxicity ratio in relation to selectivity to ergosterol membranes. Antibiotics 2023; 12(1):151.
52. Tian H, Ketkar R, Tao P. ADMETboost: a web server for accurate ADMET prediction. J Mol Model 2022; 28(12):408.
53. Vazirian M, Faramarzi MA, Ebrahimi SES, Esfahani HRM, Samadi N, Hosseini SA, Asghari A, Manayi A, Mousazadeh SA, Asef MR, Habibi E. Antimicrobial effect of the Lingzhi or Reishi medicinal mushroom, Ganoderma lucidum (higher Basidiomycetes) and its main compounds. Int J Med Mushrooms 2014; 16(1).
54. Villares A, García-Lafuente A, Guillamon E, Ramos A. Identification and quantification of ergosterol and phenolic compounds occurring in Tuber spp. truffles. J Food Compos Anal 2012; 26(1-2):177.
55. Wiederstein M, Sippl MJ. ProSA-web: interactive web service for the recognition of errors in three-dimensional structures of proteins. NAR 2007; 35(2):407.
56. Woolhouse ME, Brierley L, McCaffery C, Lycett S. Assessing the epidemic potential of RNA and DNA viruses. Emerg Infect Dis 2016; 22(12):2037.
57. Yamamoto E, Akimoto T, Mitsutake A, Metzler R. Universal relation between instantaneous diffusivity and radius of gyration of proteins in aqueous solution. PRL 2021; 126(12):128101.
58. Yang H, Tong J, Lee CW, Ha S, Eom SH, Im YJ. Structural mechanism of ergosterol regulation by fungal sterol transcription factor Upc2. Nat. Commun 2015; 6(1):6129.
59. Zahmatyar M, Fazlollahi A, Motamedi A, Zolfi M, Seyedi F, Nejadghaderi SA, Sullman MJ, Mohammadinasab R, Kolahi AA, Arsh S, Safiri S. Human monkeypox: history, presentations, transmission, epidemiology, diagnosis, treatment, and prevention. Front Med 2023; 10:1157670.
60. Zhou B, Liang X, Feng Q, Li J, Pan X, Xie P, Yang Z. Ergosterol peroxide suppresses influenza A virus-induced pro-inflammatory response and apoptosis by blocking RIG-I signaling. Eur. J. Pharmacol. 2019; (860): 172543.